A Relaxation Strategy for the Optimization of Airborne Wind Energy Systems

Sébastien Gros, M. Zanon and Moritz Diehl

Abstract— **Optimal control is recognized by the Airborne Wind Energy (AWE) community as a crucial tool for the development of the AWE industry. More specifically, the optimization of AWE systems for power generation is required to achieve the performance needed for their industrial viability. Models for AWE systems are highly nonlinear coupled systems. As a result, the optimization of power generation based on Newton-type techniques requires a very good initial guess. Such initial guess, however, is generally not available. To tackle this issue, this paper proposes a homotopy strategy based on the relaxation of the dynamic constraints of the optimization problem. The relaxed problem differs from the original one only by a single parameter, which is gradually modified to obtain the solution to the original problem.**

Keywords **: airborne wind energy, optimal control, non-convex optimization, flight control**

I. INTRODUCTION

To overcome the major difficulties posed by the exponentially growing size and mass of conventional wind turbine generators [12], [5], the Airborne Wind Energy (AWE) paradigm proposes to get rid of the structural elements not directly involved in power generation. An emerging consensus recognizes crosswind flight as the most efficient approach to perform power generation [13]. Crosswind flight consists in extracting power from the wind field by flying a rigid or flexible wing tethered to the ground at a high velocity across the wind direction. Power can be generated in two ways: (a) by performing a cyclical variation of the tether length, together with cyclical variation of the tether tension, a strategy labeled as *pumping* or (b) by using on-board turbines, transmitting the power to the ground via the tether. In this paper, the pumping strategy is considered.

Because it involves a much lighter structure, a major advantage of power generation based on crosswind flight over conventional wind turbines is that higher altitude can arguably be reached, hence tapping into wind resources that cannot be accessed by conventional wind turbines.

While the potential efficiency of the principle is established in theory, a major research effort is still required to address the many engineering difficulties posed by its implementation, and to achieve its industrial development. In particular, it is widely recognized in the AWE community that the industrial viability of the technology will require the optimization of the power generation.

S. Gros, M. Zanon and M. Diehl are with the Optimization in Engineering Center (OPTEC), K.U. Leuven, Kasteelpark Arenberg 10, B-3001 Leuven-Heverlee, Belgium. sgros@esat.kuleuven.be, mario.zanon@esat.kuleuven.be, moritz.diehl@esat.kuleuven.be

Though optimization is currently used by the AWE community to address simple design problems, a significant research effort is still needed to develop tools that can be reliably used for the optimization of AWE systems based on complex, high-fidelity models. Such models yield strongly nonlinear dynamics, resulting in strongly non-convex optimal control problems (OCPs). Solving non-convex OCPs using derivative-based optimization techniques requires initial guesses that are close to feasibility. However, in practice, a good initial guess is seldom available.

To tackle that issue, this paper proposes to solve a modified problem, where the dynamic constraints resulting from the physical model are relaxed by the introduction of fictitious forces and moments at critical stages of the dynamics. This strategy allows to dramatically reduce the model nonlinearities and couplings. As a result, Newton-type techniques converge reliably for the relaxed problem even with a poor, infeasible initial guess. The discrepancy between the dynamic constraints of the relaxed problem and of the physical model can be adjusted via a single parameter. Starting from the fully relaxed problem, a homotopy procedure is then applied, where the relaxation parameter is gradually modified so that at the end of the homotopy the dynamic constraints of the relaxed problem match the original ones.

This paper is organized as follows. Section II presents a model for AWE systems for which solving the optimal power-generation problem directly is very challenging. Section III presents the power optimization problem, and proposes a systematic, explicit technique to develop an initial guess. Section IV presents the proposed relaxed problem and the homotopy procedure. As an illustrative example, Section V applies the proposed technique for the construction of two power-generating trajectories. Section VI presents conclusions and plans for future work.

Contribution of the paper: a homotopy technique for the construction of optimal power-generating trajectories for complex AWE systems by Newton-type optimization.

II. MODEL FOR AWE SYSTEM

This section proposes a model for AWE systems. While the proposed model does not include all the physical effects encountered in AWE systems, it is sufficiently complex and nonlinear to make the computation of optimal power-generation trajectories an involved problem, and was therefore chosen to test the proposed optimization strategy.

The wing is considered as a rigid body having 6 degrees of freedom (DOF). An orthonormal right-hand reference frame

E is chosen s.t. a) the wind is blowing in the E_1-direction, b) the vector E_3 is opposed to the gravitational acceleration vector g. The origin of the coordinate system coincides with the generator. The position of the wing center of mass in the reference frame E is given by the coordinate vector $p = [x,y,z]^T$. The tether is approximated as a rigid link of (time-varying) length r that constrains p to evolve on the 2-dimensional manifold $C = \frac{1}{2}\left(p^T p - r^2\right) = 0$. Such an assumption requires that the tether is always under tension. In this paper, it is assumed that the second time derivative of the tether length, i.e. $\ddot{r} \in \mathbb{R}$ is a control variable.

A right-hand orthonormal reference frame e is attached to the wing s.t. a) the basis vector e_1 spans the wing longitudinal axis, pointing in the forward direction and is aligned with the wing chord, b) the basis vector e_3 spans the vertical axis, pointing in the upward direction. The origin of e is attached to the center of mass of the wing. In the following, the vectors $e_{1,2,3}$ are given in E (see Fig. 2). The description of the wing attitude is given by the rotation matrix R.

$$R = \left[\begin{array}{ccc} e_1 & e_2 & e_3 \end{array}\right],$$

Because the set of coordinates $\{x,y,z\}$ describes the position of the center of mass of the wing, the translational dynamics and the rotational dynamics are separable, and the wing rotational dynamics reduce to:

$$\dot{R} = R\omega_\times, \quad J\dot{\omega} + \omega \times J\omega = T, \quad \langle e_i, e_j \rangle_{t=0} = \delta_{ij}, \qquad (1)$$

where $\omega_\times \in SO(3)$ is the skew matrix yielded by the angular velocity vector ω, and $T \in \mathbb{R}^3$ is the moment vector in e. Because $\langle e_i, \dot{e}_j \rangle = 0$, the orthonormality conditions $\langle e_i, e_j \rangle = \delta_{ij}$ are preserved by the dynamics (1). Yet, for long integration times, a correction of the numerical drift of the orthonormality of R may be needed (see e.g [9]).

The kinetic and potential energy functions associated to the translational dynamics of the wing read:

$$\mathcal{T}_\mathrm{W} = \tfrac{1}{2} M_\mathrm{W} \dot{X}^T \dot{p}, \quad \mathcal{V}_\mathrm{W} = M_\mathrm{W} g z,$$

where M_W is the mass of the wing. The kinetic and potential energy functions associated to the translational dynamics of the tether read:

$$\mathcal{T}_\mathrm{T} = \tfrac{1}{2}\int_0^1 \sigma^2 \dot{p}^T \dot{p} \mu r d\sigma = \tfrac{1}{6}\mu r \dot{p}^T \dot{p}, \quad \mathcal{V}_\mathrm{T} = \tfrac{1}{2}\mu r g z,$$

where μ is the tether linear density. The Lagrangian associated to the translational dynamics of the system reads:

$$\mathcal{L} = \mathcal{T}_\mathrm{W} + \mathcal{T}_\mathrm{T} - \mathcal{V}_\mathrm{W} - \mathcal{V}_\mathrm{T} - \lambda C,$$

where λ is the Lagrange multiplier associated to the algebraic constraint C. With $\mathcal{V} = \mathcal{V}_\mathrm{W} + \mathcal{V}_\mathrm{T}$, using the Lagrange equation

$$\frac{d}{dt}\frac{\partial \mathcal{L}}{\partial \dot{p}} - \frac{\partial \mathcal{L}}{\partial p} = F,$$

the system translational dynamics are given by the following index-3 DAE:

$$m\ddot{p} + \dot{m}\dot{p} + \mathcal{V}_p + \lambda p = F, \quad C = 0, \qquad (2)$$

where $\mathcal{V}_p^T = \nabla_p \mathcal{V} = \left[\begin{array}{ccc} 0 & 0 & \left(M_\mathrm{W} + \frac{1}{2}\mu r\right) g \end{array}\right]$, F is the vector of generalized forces associated to $\{x,y,z\}$ and $m = M_\mathrm{W} + \frac{1}{3}\mu r$.

As an alternative to using (2), an index-reduction reformulates (2) as an index-1 DAE. Using $\ddot{C}(t) = 0, \dot{C}(t=0) = 0, C(t=0) = 0$, the resulting index reduction of (2) yields the following index-1 DAE and consistency conditions:

$$\begin{aligned} \left[\begin{array}{cc} m\cdot I_3 & p \\ p^T & 0 \end{array}\right]\left[\begin{array}{c} \ddot{p} \\ \lambda \end{array}\right] &= \left[\begin{array}{c} F - \mathcal{V}_p - \dot{m}\dot{p} \\ \dot{r}^2 + r\ddot{r} - \dot{p}^T\dot{p} \end{array}\right], \qquad (3) \\ C(t=0) &= \frac{1}{2}\left(p^T p - r^2\right)_{t=0} = 0, \\ \dot{C}(t=0) &= \left(p^T\dot{p} - r\dot{r}\right)_{t=0} = 0, \end{aligned}$$

where I_3 is the 3×3 identity matrix and F the force applied at the center of mass of the wing. The force in the tether and the mechanical power extracted from the wing are readily given by:

$$F_\mathrm{T} = \|\lambda p\| = \lambda r, \qquad \dot{E} = F_\mathrm{T}\dot{r} = \lambda r\dot{r}. \qquad (4)$$

Because a Cartesian coordinate system is used, the generalized forces F in (3) are given by the sum of the forces acting at the wing center of mass, given in frame e. Introducing the relative velocity v, i.e. the velocity of the wing w.r.t. the air mass given in the reference frame E by:

$$v = \left[\begin{array}{ccc} \dot{x} - W_1 & \dot{y} - W_2 & \dot{z} - W_3 \end{array}\right]^T,$$

where $W \in \mathbb{R}^3$ is the local wind velocity field, the norms of the lift and drag forces are given by [15]:

$$\|F_\mathrm{L}\| = \frac{1}{2}\rho A C_\mathrm{L}\|v\|^2, \qquad \|F_\mathrm{D}\| = \frac{1}{2}\rho A C_\mathrm{D}\|v\|^2,$$

where C_L and C_D are the lift and drag coefficient, respectively, ρ is the air density, and A the wing surface.

The lift force is orthogonal to the relative velocity v. Moreover, it is assumed in this model that the lift force is orthogonal to the wing transversal axis spanned by e_2, therefore the lift force is collinear to the vector $v \times e_2$, which is normed to $\|v\|$. The drag force is defined as collinear and opposed to the relative velocity v. The lift and drag forces, F_L and F_D acting on the wing are therefore given by:

$$F_\mathrm{L} = \frac{1}{2}\rho A C_\mathrm{L}\|v\|\left(v \times e_2\right), \qquad F_\mathrm{D} = -\frac{1}{2}\rho A C_\mathrm{D}\|v\|v. \qquad (5)$$

In this model, it is assumed that the lift and drag coefficients C_L and C_D depend on the angle of attack α and side-slip angle β only. For some range $\alpha_{\min} \le \alpha \le \alpha_{\max}$ and $-\beta_{\max} \le \beta \le \beta_{\max}$, C_L and C_D are well approximated by [15], [6]:

$$C_\mathrm{L} = C_\mathrm{L}^0 + C_\mathrm{L}^\alpha \alpha, \qquad C_\mathrm{D} = C_\mathrm{D}^0 + C_\mathrm{D}^\alpha \alpha^2 + C_\mathrm{D}^\beta \beta^2,$$

It is assumed here that the reference frame of the wing is chosen such that $\alpha = 0$ corresponds to the minimum drag. The proposed quadratic dependence of C_D on β arises from the symmetry of the system; note that [15] neglects this contribution, while [6] proposes a linear dependence w.r.t. $|\beta|$.

Defining $v = [v_1, v_2, v_3]^T$ as the coordinate vector of the relative velocity v projected in the wing frame e, i.e.: $v = R^T v$, for small angles α and β can be approximated by [15]:

$$\alpha = -\tan\left(\frac{v_3}{v_1}\right) \approx -\frac{v_3}{v_1}, \quad \beta = \tan\left(\frac{v_2}{v_1}\right) \approx \frac{v_2}{v_1}.$$

Assuming a laminar wind flow with a logarithmic wind shear model blowing in the uniform x-direction, $W = [u, v, w]$ is given by [14]:

$$u(z) = u_0 \frac{\log(z/z_r)}{\log(z_0/z_r)}, \quad v = w = 0 \tag{6}$$

where $W_0 \in \mathbb{R}$ is the wind velocity at altitude z_0 and z_r is the ground roughness. For the sake of simplicity, in this paper only the wind along the x-axis is considered.

In this paper, the approximate tether drag model proposed in [10] is used. The tether drag is lumped into a single equivalent force F_{T}^D (projected in frame e) acting at the wing center of mass (see [10]) given by:

$$F_{\mathrm{T}}^D = -\frac{1}{8}\rho D_{\mathrm{T}} C_{\mathrm{T}} r \| [v]_e - \dot{r} e_r \| ([v]_e - \dot{r} e_r),$$

where $e_r = r^{-1} \begin{bmatrix} x, & y, & z \end{bmatrix}^T$, D_{T} is the tether diameter, and C_{T} the tether drag coefficient. The sum of the forces F in (3) acting at the wing center of mass is given by $F = F_{\mathrm{A}} + F_{\mathrm{T}}^D$.

The vector of aerodynamic moment T_{A} is given by:

$$T_{\mathrm{A}} = \frac{1}{2}\rho A \|v\|^2 \begin{bmatrix} C_{\mathrm{R}} \\ C_{\mathrm{P}} \\ C_{\mathrm{Y}} \end{bmatrix} \tag{7}$$

where

$$\begin{aligned} C_R &= -D_{\mathrm{R}}\omega_1 - A_{\mathrm{R}}\omega_3 && + C_{\mathrm{R}}^{\mathrm{a}} u_{\mathrm{a}} \\ C_P &= && C_{\mathrm{P}}\alpha + C_{\mathrm{P}}^{\mathrm{T}}\alpha_{\mathrm{T}} + C_{\mathrm{P}}^{\mathrm{e}} u_{\mathrm{e}} \\ C_Y &= A_{\mathrm{Y}}\omega_1 && + C_{\mathrm{Y}}^{\mathrm{T}}\beta_{\mathrm{T}} + C_{\mathrm{Y}}^{\mathrm{r}} u_{\mathrm{r}} \end{aligned}$$

and α_{T}, β_{T} are the tail angle of attack and side-slip angle, given by:

$$\alpha_{\mathrm{T}} = -\frac{v_3 + L_{\mathrm{T}}\omega_2}{v_1}, \qquad \beta_{\mathrm{T}} = \frac{v_2 - L_{\mathrm{T}}\omega_3}{v_1}$$

where L_{T} is the tail effective length.

In the following, $\mathcal{U} = [\ddot{r}, \dot{u}_{\mathrm{a}}, \dot{u}_{\mathrm{e}}, \dot{u}_{\mathrm{r}}]^T \in \mathbb{R}^4$ are the system control inputs, and $\mathcal{X} = \left[x, y, z, \dot{x}, \dot{y}, \dot{z}, e_1^T, e_2^T, e_3^T, \omega_1, \omega_2, \omega_3, r, \dot{r}, u_{\mathrm{a}}, u_{\mathrm{e}}, u_{\mathrm{r}}\right]^T \in \mathbb{R}^{23}$ are the system states.

A. System Constraints

We use the following control input and state bounds:

$$-5\,\mathrm{m/s^2} \leq \ddot{r} \leq 5\,\mathrm{m/s^2}, \tag{8}$$

$$-10\,\mathrm{m/s} \leq \dot{r} \leq 10\,\mathrm{m/s}. \tag{9}$$

In addition, in order to keep the system in the region where the model assumptions are valid, the following path constraints need to be considered:

$$-1 \leq C_{\mathrm{L}}(\mathcal{X}, W_0) \leq 1, \quad \lambda(\mathcal{X}, W_0) \leq 0. \tag{10}$$

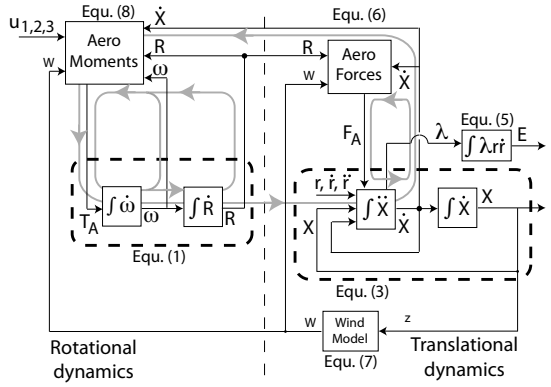

Fig. 1. Architecture of the system dynamics. The feedback loops introduced by the aerodynamics are highlighted using the light-grey arrows.

Constraint $\lambda \leq 0$ is required to keep the tether under tension, and constraint $-1 \leq C_{\mathrm{L}} \leq 1$ is required to keep the wing in the linear-lift region [15]. Note that the actual bounds on the linear-lift region depend on the wing used.

B. System architecture

A visualization of the architecture of the system dynamics is given in Fig. 1. Airborne applications are typically a chain of four nonlinear integrators, with several feedback loops occurring at different stages of the chain. The feedback loops result from the aerodynamic forces and moments, which are strongly nonlinear functions of the state of the system. The dynamics resulting from the interaction of the integrators with the aerodynamic feedback loops are highly coupled, and strongly nonlinear.

III. Power optimization

A. Power optimization problem

The optimization of power generation can be formulated as the following periodic optimization problem:

$$\mathcal{P}_{\mathrm{E}}: \min_{\mathcal{X},\mathcal{U},E,\lambda,T} \quad \frac{E(T)}{T} \tag{11}$$

$$\text{s.t.} \quad (1),\ (3),\ (4)$$

$$F = F_{\mathrm{A}},\ T = T_{\mathrm{A}} \tag{12}$$

$$\lambda \leq 0, \quad 0 \leq C_{\mathrm{L}} \leq 1 \tag{13}$$

$$\mathcal{X}(T) = \mathcal{X}(0), \tag{14}$$

$$C(\mathcal{X}(0)) = 0, \quad \dot{C}(\mathcal{X}(0)) = 0, \tag{15}$$

$$\langle e_i, e_j \rangle_{t=0} = \delta_{ij}, \quad i = 1,2,3,\ j \geq i, \tag{16}$$

Because the periodicity constraints (14) together with the consistency conditions (15)-(16) are redundant, some constraints must be removed from the periodic optimization problem (11)-(16). In this paper, the periodicity constraints on the states r and $\dot{r}$ were removed from (14), and only the leading terms $\mathbf{1}_i^T e_i(0) = \mathbf{1}_i^T e_i(T),\ i = 1,2,3$ were considered for the periodicity of R, with $[\mathbf{1}_i]_j = \delta_{ij},\ j = 1,2,3$.

B. Initial guess

For a practitioner, the a priori knowledge of the optimal trajectory of a specific AWE system is likely to be limited to its topology (e.g. circular or eight) and an educated guess of

some variables such as the wing velocity, the cable length, the turn radius, and the operational altitude. We therefore suggest in this paper to develop an initial guess for problem (11)-(16) based on such limited information only.

Because it is strongly nonlinear and because the dynamics are unstable, problem (11)-(16) is best treated using simultaneous optimization techniques [1]. In a simultaneous optimization framework, the problem is discretized on a time grid t_k, $k = 0,...,N_T$, and the states at each time t_k introduced as decision variables in the resulting Nonlinear Program.

From an arbitrary guess of the wing position over time $p_0(t)$, with $p_0(0) = p_0(T)$ and $C(p_0(t)) = 0$, $\forall t \in [0,T]$ the states are initialized at the time instants t_k such that:

1) the wing longitudinal axis e_1 is aligned with the wing absolute velocity $\dot{p}_0$. The angle of attack α is yielded by the component of the wing relative velocity due to the wind only, and is therefore small if the absolute velocity is chosen reasonably high.
2) the wing vertical axis e_3 is aligned with the tether, such that the lift mainly acts in the direction of the tether axis
3) the wing angular velocity ω is initialized by taking the numerical derivative of the pose of the wing R between the successive times t_k
4) the tether length is fixed, the wing control surfaces are neutral

These requirements can be formally stated as follows:

$$
\begin{aligned}
& e_1(t_k) = \left(\|\dot{p}_0\|^{-1}\dot{p}_0\right)_{t=t_k}, \quad k = 0,...,N_T-1 \qquad (17)\\
& e_3(t_k) = \left(r_0^{-1}\,p_0\right)_{t=t_k}, \quad e_2(t_k) = e_3(t_k)\times e_1(t_k),\\
& \omega(t_k) = \frac{N}{T}\log\left(R(t_k)^T R(t_{\mathrm{mod}(k+1,N)})\right)_{\times^{-1}},\\
& r(t_k) = r_0,\ \dot{r}(t_k) = 0,\ u_1(t_k) = 0,\ u_2(t_k) = 0,\ u_3(t_k) = 0,
\end{aligned}
$$

where $A_{\times^{-1}} \in \mathbb{R}^3$ is the vector yielded by the skew matrix $A \in SO(3)$.

Solving problem (11)-(16) with the initial guess (17) has been attempted using a) collocation-based discretization of problem $\mathcal{P}_{\mathrm{E}}$ [2] and the NLP solver Ipopt [16], and b) using the software ACADO [11] based on Multiple-Shooting [3] and Sequential Quadratic Programming (SQP) [4]. Both attempts have lead to the failure of the NLP solvers at a point where feasibility cannot be improved. The failure occured regardless of the number of shooting nodes or collocation points tested. Though alternative strategies can be considered to explicitly compute an initial guess for problem (11)-(16), none have been found that allow for a reliable convergence of Newton-type methods for problem (11)-(16). To tackle that issue, the following section presents an alternative based on a relaxed optimization problem, that allows for a refinement of the initial guess (17) through a homotopy procedure.

IV. Relaxed problem

A. Opening the feedback loops

As pointed out in Section II-B, the nonlinearities of the model dynamics are mainly due to the feedback loops introduced by the aerodynamic forces and torques. In contrast, a system where these feedback loops are open (see Fig. 3) is decoupled and mildly nonlinear. This observation is exploited here for developing a relaxed dynamic model where the feedback loops can be fully open and then progressively closed. This feature is then exploited to run a homotopy strategy on the initial guess (17). Consider the following representation of the dynamics of N subsystem through the functions g_i, i.e.:

$$
f_i(\dot{x}_i, x_i, u_i, z_i) = 0, \qquad z_i = g_i(x), \qquad i = 1,...,N \qquad (18)
$$

where $x^T = \begin{bmatrix} x_1^T & \dots & x_N^T \end{bmatrix}$ and g_i are typically sparse functions of x. We suggest here to open the feedback loops by relaxing the algebraic constraint in (18).

1) Profile closing :

$$
\begin{aligned}
& f_i(\dot{x}_i, x_i, u_i, z_i) = 0, \qquad z_i - g_i(x) = P_i(t,\alpha_i) \qquad (19)\\
& \|P(t_k,\alpha_i)\|_p \le \gamma^{-1} - 1, \quad k = 1,...,N_T
\end{aligned}
$$

where p is any appropriate norm, $P_i(t,\alpha_i)$ is a function of time parametrized by $\alpha_i \in \mathbb{R}^n$, and $\gamma \in]0,1]$. Using (19), a rich parametrization of $P_i(t,\alpha_i)$ is required to remove the couplings $z_i = g_i(x)$. In a collocation framework [2], feasibility can be achieved for all values of γ by reusing for $P_i(t,\alpha_k)$ the polynomials and the time grid used for setting up the collocation scheme, and the norm constraints enforced on the collocation nodes only. The resulting NLP is then a large-scale problem, which is typically best treated using interior-point techniques [17]. In a multiple-shooting framework [3] where the discretization of the OCP is based on a much smaller set of decision variables than in a collocation framework, a high-order parametrization of $P_i(t,\alpha_i)$ may not be desired. An alternative strategy is proposed next.

2) Gain closing : an alternative approach to (IV-A.1) consists in progressively introducing the feedback-loops in the system dynamics through adjustable gains, i.e. using:

$$
f_i(\dot{x}_i, x_i, u_i, z_i) = 0, \quad z_i = \gamma g_i(x) + (1-\gamma)P_i(t,\alpha_i) \qquad (20)
$$

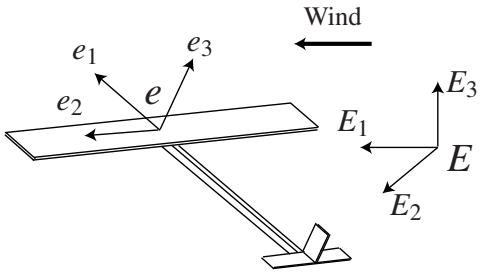

Fig. 2. Schematic of the reference frames E and e.

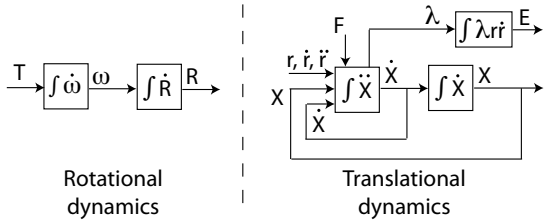

Fig. 3. Dynamic model without aerodynamic feedback loops.

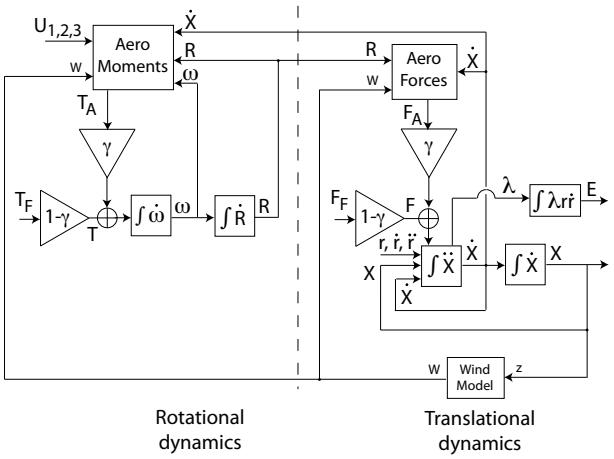

Fig. 4. Dynamic model with relaxation strategy (IV-A.2). The feedback loops can be opened and closed by changing the value of parameter γ.

where $\gamma \in [0,1]$. Since for $\gamma = 0$ the equalities $z_i = P_i(t,\alpha_i)$ hold, a high-order parametrization of is not needed to remove the couplings $z_i = g_i(x)$, and the variables z_i are controlled via the corresponding α_i.

B. Relaxed problem

In this paper, the relaxation strategy IV-A.2 is implemented (see Fig. 4). The relaxed problem aims at refining the initial guess (17) to obtain a feasible trajectory close to the prototype trajectory $p_0(t)$ used to build (17). Defining the set of decision variables $\mathcal{W} = [\mathcal{X}\ \mathcal{U}\ \lambda\ F_{\mathrm{F}}\ T_{\mathrm{F}}\ \gamma]$, the proposed relaxed problem reads:

$$\mathcal{P}(p_{\mathrm{H}}): \min_{\mathcal{W}} \int_0^T \left(\|\mathcal{X}_k - \bar{\mathcal{X}}_k\|_Q^2 + \|\mathcal{U}_k - \bar{\mathcal{U}}_k\|_R^2\right) dt$$

$$s.t. \quad (1),\ (3),\ (13)-(16)$$

$$\begin{bmatrix} F \\ T \end{bmatrix} - \gamma \begin{bmatrix} F_{\mathrm{A}} \\ T_{\mathrm{A}} \end{bmatrix} - (1-\gamma) \begin{bmatrix} F_{\mathrm{F}} \\ T_{\mathrm{F}} \end{bmatrix} = 0 \qquad (21)$$

$$\gamma - p_{\mathrm{H}} = 0 \qquad (22)$$

The following homotopy procedure was applied to problem $\mathcal{P}$ for some $N_{\mathrm{H}} \in \mathbb{N}$ sufficiently large:

Algorithm 1: (Homotopy)
Initialization: states (17), $p_{\mathrm{H}} := 0$, $\mathrm{TOL}_0 > \mathrm{TOL}_{\mathrm{END}} > 0$
While $p_{\mathrm{H}} \leq 1$ **do:**
1. solve $\mathcal{P}(p_{\mathrm{H}})$ to tolerance TOL_0
2. $p_{\mathrm{H}} := p_{\mathrm{H}} - \frac{1}{N_{\mathrm{H}}}$

end while.
Solve $\mathcal{P}_{\mathrm{E}}$ to $\mathrm{TOL}_{\mathrm{END}}$.

The homotopy parameter p_{H} is embedded [7] in problem $\mathcal{P}$ by introducing the decision variable γ and the constraint (22). As a result, for a given value of p_{H} the parametric Quadratic Program (QP) obtained at a solution of problem $\mathcal{P}(p_{\mathrm{H}})$ provides a linear predictor for the next homotopy step, hence improving the convergence of the Newton scheme. Once $\mathcal{P}(0)$ has been solved to a reasonable degree of accuracy TOL_0, for N_{H} chosen sufficiently large, a single full Newton step can be sufficient to update the solution. However, if the homotopy step size is not adjusted to ensure that the accuracy of the solution remains sufficient throughout the homotopy, more than one (not necessarily full) Newton steps may be needed. In the proposed implementation, the dynamics in problem $\mathcal{P}$ and $\mathcal{P}_{\mathcal{E}}$ where discretized using multiple-shooting [3], and the resulting NLP tackled via the SQP method implemented in the software ACADO [11]. The primal active set QP solver qpOASES [8] was used to solve the underlying Quadratic Problems.

TABLE I
MODEL PARAMETERS

Parameter	Value	Unit
m_{A}, A	$5\cdot10^3$, 100	(kg), (m^2)
$\mathrm{diag}(I)$	$\begin{bmatrix}4.4\cdot10^3 & 2.1\cdot10^3 & 6.2\cdot10^3\end{bmatrix}$	($\mathrm{kg}\cdot\mathrm{m}^2$)
α_0^{t}, L_{T}	-10, 5	(deg), (m)
C_{L}^{α}	3.82	-
C_{D}^0, C_{D}^{α}, C_{D}^{β}	10^{-2}, 0.25, 0.1	-
$C_{\mathrm{R}}^{\mathrm{u}}$, $C_{\mathrm{R}}^{\mathrm{l}}$, C_{R}^{3}	0.1, -4, 1	-
$C_{\mathrm{P}}^{\mathrm{u}}$, $C_{\mathrm{P}}^{\mathrm{l}}$, C_{P}^{α}	0.1, 7.5, 1	-
$C_{\mathrm{Y}}^{\mathrm{u}}$, $C_{\mathrm{Y}}^{\mathrm{l}}$, C_{Y}^{r}	0.1, 0.1, 7.5	-
$z_{\mathrm{r}}, z_0, \rho$	10^{-2}, 100, 1.23	(m),(m),($\mathrm{kg}\cdot\mathrm{m}^{-3}$)

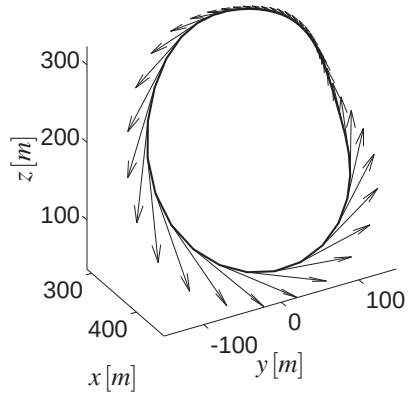

Fig. 5. 3D trajectory resulting from initial guess (23). The arrows are the wing velocity.

V. ILLUSTRATIVE EXAMPLE

Two common types of trajectories for AWE systems are considered. The first is a circular trajectory, a topology that is often preferred in practice for its simplicity, but for which a swivel mechanism is required to avoid the winding of the tether. The second trajectory is a lying eight, for which the problem of tether winding is avoided, but which requires strong angular accelerations $\dot{\omega}$ to be performed.

A. Circular trajectory

The relaxed optimization problem $\mathcal{P}$ was initialized using:

$$\delta_k = 2k\pi/N, \quad \psi_k = \psi_{\max}\sin(\delta_k) + \psi_0, \quad \theta_k = \theta_{\max}\cos(\delta_k),$$

$$p(\psi_k, \theta_k, r) = r \begin{bmatrix} \cos(\psi_k)\cos(\theta_k) \\ \sin(\theta_k) \\ \cos(\theta_k)\sin(\psi_k) \end{bmatrix} \qquad (23)$$

for $k = 0,\ldots,N-1$, where r, $\psi_{\max}$, ψ_0 and $\theta_{\max}$ must be chosen by the user. The state and input guess was computed using (17). The 3D trajectories are reported in Fig. 5.

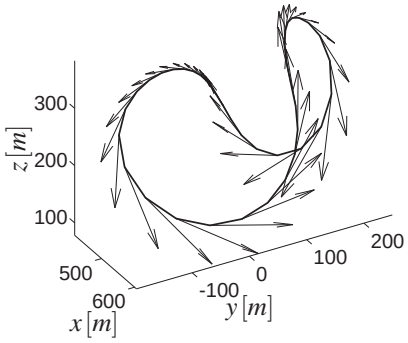

Fig. 6. 3D trajectory resulting from initial guess (24). The arrows are the wing velocity.

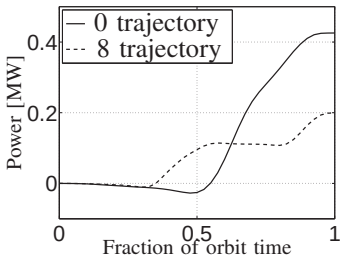

Fig. 7. Time evolution of the generated power for both trajectories.

B. Lying eight trajectory

The relaxed optimization problem $\mathcal{P}$ was initialized using:

$$\begin{aligned} \delta_k &= 2k\pi/N, \quad \psi_k = \psi_{\max}\sin(2\delta_k) + \psi_0, \\ \theta_k &= \quad \theta_{\max}\left(\cos(2\delta_k) - 1\right), \quad \delta_k \in [0, \pi[, \\ \theta_k &= -\theta_{\max}\left(\cos(2\delta_k) - 1\right), \quad \delta_k \in [\pi, 2\pi[, \end{aligned} \tag{24}$$

for $k = 0, \ldots, N-1$. The state and input guess was computed using (17). The 3D trajectories are reported in Fig. 6.

The average power generated throughout orbits are reported for both trajectories in Fig. 7. The arguably modest optimal power results from the dynamics of the wing, which were not optimized for AWE, and from the choice of having only one orbit per pumping cycle, instead of several. This results underlines the necessity to optimize the wing for power generation, and for investigating the ideal number of orbit per pumping cycle. This investigation is the object of current work.

VI. Conclusion & Future work

This paper has proposed a reliable homotopy strategy to compute optimal power-generating trajectories for Airborne Wind Energy (AWE) systems. Because the dynamics of models for AWE systems are highly nonlinear, and because only poor initial guesses are usually available, attempting to solve the power-generation problem directly typically leads to the failure of the NLP solver, which stops prematurely at a point where feasibility cannot be improved.

The nonlinearities of AWE systems come chiefly from the feedback loops introduced by the aerodynamic forces and moments. This paper proposes to relax the dynamic constraints associated to the model of the AWE system by opening the aerodynamic feedback loops. The relaxed problem can be reliably solved, and a solution to the original problem designed by running a homotopy that gradually closes the feedback loops.

The strategy was successfully tested on a classical, complex model for AWE systems for two different type of trajectories. Future work will test the technique on high-fidelity models, where tether dynamics and complex aerodynamic effects are taken into account. Heuristics to compute an adaptive step size for the homotopy parameter p_{H} will be considered in order to minimize the amount of computations required in the homotopy loop.

VII. Acknowledgments

This research was supported by Research Council KUL: PFV/10/002 Optimization in Engineering Center OPTEC, GOA/10/09 MaNet; Flemish Government: IOF/KP/SCORES4CHEM, FWO: PhD/postdoc grants and projects: G.0320.08 (convex MPC), G.0377.09 (Mechatronics MPC); IWT: PhD Grants, projects: SBO LeCoPro; Belgian Federal Science Policy Office: IUAP P7 (DYSCO, Dynamical systems, control and optimization, 2012-2017); EU: FP7-EMBOCON (ICT-248940), FP7-SADCO (MC ITN-264735), ERC ST HIGHWIND (259 166), Eurostars SMART, ACCM.

References

[1] L.T. Biegler. An overview of simultaneous strategies for dynamic optimization. *Chemical Engineering and Processing*, 46:1043–1053, 2007.

[2] L.T. Biegler. *Nonlinear Programming*. 2010.

[3] H.G. Bock and K.J. Plitt. A multiple shooting algorithm for direct solution of optimal control problems. In *Proceedings 9th IFAC World Congress Budapest*, pages 242–247. Pergamon Press, 1984.

[4] P.T. Boggs and J.W. Tolle. Sequential Quadratic Programming. *Acta Numerica*, pages 1–51, 1995.

[5] E. A. Bossanyi. Further Load Reductions with Individual Pitch Control. *Wind Energy*, 8:481–485, 2005.

[6] Michael V. Cook. *Flight Dynamics Principles*. Elsevier Science, 2007.

[7] Diehl, M. and Bock, H.G. and Schlöder, J.P. Real-Time Iterations for Nonlinear Optimal Feedback Control. In *Decision and Control, 2005 and 2005 European Control Conference. CDC-ECC '05. 44th IEEE Conference on*, pages 5871 – 5876, 2005.

[8] H.J. Ferreau, C. Kirches, A. Potschka, H.G. Bock, and M. Diehl. qpOASES: A parametric active-set algorithm for quadratic programming. *Mathematical Programming Computation*, 2012. (submitted).

[9] S. Gros, R. Quirynen, and M. Diehl. Aircraft Control Based on Fast Nonlinear MPC & Multiple-shooting. In *Conference on Decision and Control*, 2012.

[10] B. Houska and M. Diehl. Optimal Control for Power Generating Kites. In *Proc. 9th European Control Conference*, pages 3560–3567, Kos, Greece,, 2007. (CD-ROM).

[11] B. Houska, H.J. Ferreau, and M. Diehl. ACADO Toolkit – An Open Source Framework for Automatic Control and Dynamic Optimization. *Optimal Control Applications and Methods*, 32(3):298–312, 2011.

[12] J.H. Laks, L.Y. Pao, and A.D. Wright. Control of Wind Turbines: Past, Present, and Future. In *American Control Conference*, pages 2096–2103, 2009.

[13] M.L. Loyd. Crosswind Kite Power. *Journal of Energy*, 4(3):106–111, July 1980.

[14] Manwell, J. F., McGowan, J. G. and Rogers, A. L. *Wind Energy Explained: Theory, Design and Application, Second Edition*. John Wiley & Sons, Ltd, Chichester, UK, 2009.

[15] Pamadi. *Performance, Stability, Dynamics, and Control of Airplanes*. American Institute of Aeronautics and Astronautics, Inc., 2003.

[16] A. Wächter and L. Biegler. IPOPT - an Interior Point OPTimizer. https://projects.coin-or.org/Ipopt, 2009.

[17] S.J. Wright. *Primal-Dual Interior-Point Methods*. SIAM Publications, Philadelphia, 1997.